Acta Technica *62* (2017), No. 6A, 355–362

Seismic Performance of large-scale reinforced concrete columns with different shear-span ratios

Jia Lei[1] Xie Yong-ping[1,*] Li Yuan[1] Bai Wen-ting[1]

Abstract. In order to study the seismic performance of large-scale reinforced concrete columns, two large size specimens are designed, including bending failure specimens and shear bond failure specimens. Utilizing 40000kN loading system, these reinforced concrete columns were test under low cycle reversed loading. Their seismic behavior is achieved, including the failure characteristic, hysteretic behavior, deformation and energy dissipation. The results show that the specimen WF-4-7-0.4 occur bending failure, and has stronger energy dissipation capacity and the deformation ability. The deformation of plastic hinge region is about 90% of the total deformation. However, specimen JF-2-7-0.4 occur shear bond failure, the hysteresis curves are narrow, and there is low energy dissipation capacity and ductility.

Key words. Large-scale specimen, reinforced concrete columns, seismic behavior, bending failure, shear bond failure.

1. Introduction

With the rapid development of the city, More and more high-rise buildings are built, and reinforced concrete columns are becoming larger and larger. Previously, in order to obtain the seismic performance of reinforced concrete column, many small scale specimens were tested due to the limitation of test conditions [1,2,3,4], therefore, very few large scale specimens, especially the high axial pressure ratio, are tested. HE et al [5] carried out 2 groups of specimens in order to study the effects of clip steel bar on failure modes of reinforced concrete columns, the cross-section size was 700mm, but axial compression ratio was only 0.05. Some reinforced

Supported by the National Natural Science Foundation of China (Fund No: 51408378) and the Natural Science Foundation of Hebei Province, China (Fund No: E2016403060 , E2015403018).

[1]College of Exploration Technology and Engineering, HeBei GEO University,Shijiazhuang 050031, China.

* Corresponding author. E-mail: axypa@163.com

concrete columns with high axial compression ratio, which cross-section size were 510mm×510mm and 450mm×650mm were tested by XIAO [6] and LV [7], respectively, but the object of study was high strength concrete. However, some large-scale columns subjected to axial compression were already tested, for example, SONG et al [8] carried out 2 groups of specimens, the largest cross-section size was 800mm, the experiment concluded that the axial compression behavior of large scale specimens are different from small-scale specimens. In addition, lots of experimental results [9,10,11,12,13,14] have shown that the compressive strength decreases as the section size increases. However, SHAMIM and MURAT [15] tested on short columns found that the ductility of the post peak decreases with the increasing specimen size.

Therefore, so far, the seismic performance of large scale columns under high axial compression ratio remains unclear. In this research, In order to understand the seismic behavior of specimens under different failure modes, such as bending failure and shear failure, experiment was carried out through 2 specimens under low cycle reversed loading. The specimens were designed with different shear-span ratio and volumetric ratio of transverse reinforced. Their seismic behavior, including the failure characteristic, hysteretic behavior, deformation and energy dissipation, were studied.

2. Experimental design

2.1. Specimens and mechanical properties of materials

The size of cross-section of 2 specimens was designed with 700mm×700mm. The volumetric ratio of transverse reinforced ρ_v was 1.89% and 0.338% respectively, shear span ratio λ was 4.39 and 2.39 respectively. Experimental axial compression ratio n was 0.4. The grade of concrete was C30. The grade of longitudinal steel bar was HRB400, its yield strength was 422 MPa. The grade of transverse reinforced was HPB300, its yield strength was 327 MPa. Details of specimens are listed in Table 1. Section size and steel bar of specimens are shown in Fig.1.

Table 1. Details of specimens

Number	$b \times h$ mm^2	H /mm	f_{cp} /MPa	c /mm	λ	n	N/kN	transverse reinforced	longitudinal steel bar	ρ_v%
WF-4-7-0.4	700 × 700	2548 + 250	30	35	4.39	0.4	5880	4 ϕ 14 @ 100	12 Φ 28	1.89
JF-2-7-0.4	700 × 700	1274 + 250	30	35	2.39	0.4	5880	2 ϕ 14 @ 280	12 Φ 28	0.338

Notes: b and h are the width and height of cross-section; The letter F is low cycle reversed loading; N is axial loading; f_{cp} is the compressive strength of concrete cubic (150 mm × 150 mm × 150 mm); actual shear span ratio $\lambda = H/h_0$, H is the height of specimen, the value in front of the plus is the height of the column, the value behind the plus is the height of the joint(fig.2). c is the thickness of concrete cover.

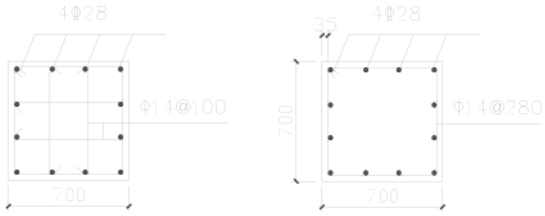

(a)First group (b)Second group

Fig. 1. Section size and steel bar of specimens

2.2. Test method and test content

2.2.1. Setup of experiment

The 40000 kN multiple function electro hydraulic servo test machine (see Fig. 2) was used to apply monotonic horizontal loading and low cycle reversed loading. The axial loading was applied to the top of the joint, which was connected to the steel beam, and the lower part was connected to the specimen to ensure that the specimen only rotation without horizontal displacement at the top. The height of joint was 250mm. The base and the equipment scooter were connected to the horizontal motion.

Before the yield status of specimen was reached, the force control method was applied in the loading process. Then, after the yield status of specimen, the displacement control method was applied until the specimen failed.

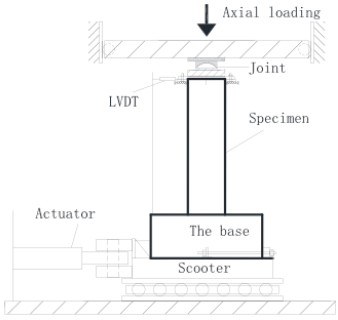

Fig. 2. Test set-up

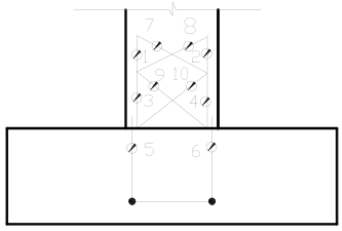

Fig. 3. Installation position of dial indicators

2.2.2. Deformation measure

The specimens were instrumented with linear variable differential transformers (LVDT) to measure horizontal deformations, as shown in Fig. 3, The scale range of LVDT was 300 mm. In order to ensure that the measured displacement was the horizontal deformation, the bar that connect LVDT was fixed with the base, the load-displacement curves of specimen were obtained. In addition, 10 dial indicators

were installed at the bottom of the column to measure bending deformation, shear deformation and bonding slip deformation of the plastic hinge region, as shown in Fig.3.

3. Test results and analysis of the first group specimens

3.1. Failure modes

When the horizontal load is applied to 2 times yield displacement, the compressive zone of specimen WF-4-7-0.4 has a long vertical crack, which is about 400mm in length. When the horizontal load is applied to 3 times yield displacement, there are no new level cracks, 6∼7 horizontal cracks were found within the range of 1.5h highly, however, there are more and more vertical cracks in the compression zone. Then the horizontal cracks of above 0.5 h are developed along the horizontal direction, and then it goes down the slope, the angle is about 45°. When 5 times yield displacement is applied on the specimens, the concrete protection layer in the pressure area of specimen is falling down, and the longitudinal bars are bent by compression. So the specimens occur bend failure, the features of final failure pattern are shown in Fig.4(a).

When the load is 750kN, a vertical crack is found in the middle of specimen JF-2-7-0.4, and extends down from the top of specimen When the horizontal load is applied to -900kN, two horizontal cracks appear in the left of specimen, which the distance to the base of specimen are 100mm and 200mm, respectively. At 900kN, a horizontal crack in the right root was about 110mm. when the horizontal displacement applied to 4 mm (Δ=4mm), there is no new crack appeared, but the horizontal crack widening and extends along the horizontal direction, and vertical cracks continue to down, two horizontal cracks of about 200mm appear in the right of specimen, which the distance to the base of specimen are 180mm and 350mm, respectively. When the horizontal displacement applied to 6 mm (Δ=6mm), a 200mm vertical crack appear in the left of specimen, and many of the diagonal cracks appear next to the initial vertical cracks. When the horizontal displacement is applied to 10mm, the vertical cracks are widened, and there are more diagonal cracks in the area around it, and the concrete is falling off. When the horizontal displacement is applied to 14mm, large area concrete quickly falls off, the specimen failure, as shown in Fig.4(b).

3.2. Load-displacement curve of specimens

The load-displacement curves of specimens are shown in Fig.5. It can be seen from the curve, the hysteresis curves of the specimen WF-4-7-0.4 is full, however, the hysteresis curve of the specimen JF-2-7-0.4 is narrow, after the peak load, the bearing capacity of the specimen fall fast and the deformation is smaller, so it has a poor ductility.

Due to the axial compression of specimens is larger, there is no obvious crack point on the skeleton curve, so the yield point, peak load point and limit displacement

(a) WF-4-7-0.4 (b) JF-2-7-0.6

Fig. 4. Final failure states of specimens

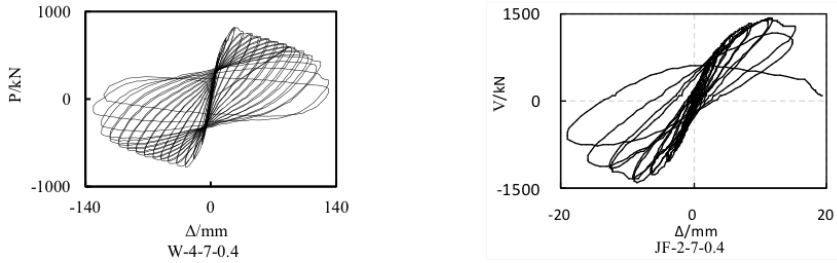

Fig. 5. Load-displacement curves of specimens

can be considered the characteristic point of the skeleton curve. Table 2 lists the test results.

Table 2. Test results of specimens

Number	Loading direction	Yield point		Peak load point		Limit displacement		ductility
		P_y/kN	Δy/mm	P_m/kN	Δm/mm	P_u/kN	Δu/mm	
WF-4-7-0.4	positive	702	17.3	823.8	26.4	700.2	58	3.58
	negative	658.4	17	780.2	28	663.1	64.8	
JF-2-7-0.4	positive	1220	6.97	1425.3	11.78	-	-	1.67
	negative	1201.9	5.17	1417.2	8.51	-	-	

3.3. The deformation composition of the WF-4-7-0.4

Fig.6 illustrates that the total deformation consists of bending deformation (Δ_f), shear deformation (Δ_s) and bonding slip deformation (Δ_{slip}). The deformation of the yield point, peak load point and limit displacement point is calculated according to the test value in Fig.3 and the following formula, and the results are shown in table 3.

$$\Delta'_F = (H - 0.5l)(\delta_1 - \delta_2)/h, \tag{1}$$

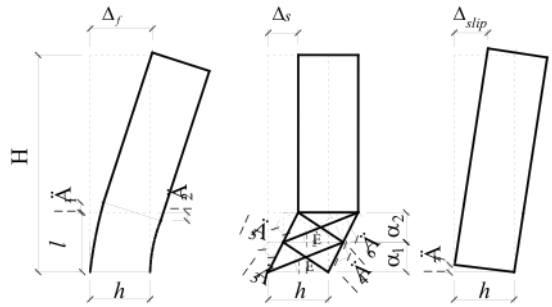

(a) Δ_f (b) Δ_s Δ_{slip}

Fig. 6. The three main deformation components

$$\begin{aligned}\Delta_s &= \frac{|\delta_3|+|\delta_4|}{2\cos\theta_1}+\frac{|\delta_5|+|\delta_6|}{2\cos\theta_2}\\ &= \frac{(|\delta_3|+|\delta_4|)\sqrt{a_1^2+h^2}}{2h}+\frac{(|\delta_5|+|\delta_6|)\sqrt{a_2^2+h^2}}{2h},\end{aligned} \tag{2}$$

$$\Delta_{slip} = \delta_7 H/h_0, \tag{3}$$

$$\Delta_f'' = \Delta - \Delta_f' - \Delta_s - \Delta_{slip}. \tag{4}$$

Where l is the height of dial indicators in the plastic hinge region. Δ_f' is the deformation of plastic hinge region l. Δ_f'' is the bending deformation of H-l range caused by fracture and elastic deformation. Δ is the level displacement specimens. $\delta_1 \sim \delta_7$ is the elongation or compression value of dial indicators.

In table 3, Δ_f is the total bending deformation of specimens, namely $\Delta_f = \Delta_f' + \Delta_f''$. Δ' is the plastic hinge region deformation caused by bending, shear and slip deformation, namely $\Delta' = \Delta_f' + \Delta_s + \Delta_{slip}$. It is can be seen form the table 3, the deformation $\Delta f'$ is about 70%∼80% of the plastic hinge region deformation Δ', and is about 60%∼70% of the total deformation Δ. The total bending deformation Δ_f is about 70%∼80% of the total deformation Δ. The plastic hinge region deformation Δ_f' is about 90% of the total deformation Δ, and the value increases as the displacement increases.

Table 3. Test results of deformation

Loading		Δ_f'/mm ((Δ_f'/Δ')/%)	Δ_s/mm ((Δ_s/Δ')/%)	Δ_{slip} /mm ((Δ_{slip}/Δ')/%	Δ_f''/mm ((Δ_f''/Δ)/%)	Δ_f'/Δ (%)	Δ_f/Δ (%)	Δ'/Δ (%)
Yield point	positive	21.45(84.7)	1.71(6.8)	2.17(8.6)	1.08(4.1)	81.2	85.3	95.9
	negative	22.69(84.5)	1.72(6.4)	2.43(9.1)	1.14(4.1)	81.1	85.2	95.9
Peak load point	positive	47.47(85.7)	3.58(6.5)	4.35(7.9)	2.59(4.5)	81.9	86.3	95.5
	negative	53.22(85.9)	4.50(7.3)	4.20(6.8)	2.88(4.4)	82.1	86.6	95.6
Limit displacement	positive	11.23(84.0)	1.05(7.9)	1.09(8.2)	0.65(4.6)	80.1	84.7	95.4
	negative	12.25(84.5)	1.11(7.7)	1.14(7.9)	0.57(3.8)	81.3	85.1	96.2

3.4. Energy dissipation capacity

The relationship between the Equivalent viscous damping coefficient h_e and the Angle θ at the top of the column is shown in Fig.7. It can be seen from the figure 7, the early loading, equivalent viscous damping coefficient of the two specimens is approximation equal, but specimens WF-4-7-0.4 have larger the deformation, thus which have a good energy dissipation capacity, and the viscous damping coefficient increases with the increase of angle, however, the energy dissipation capacity of specimen JF-2-7-0.4 is very poor.

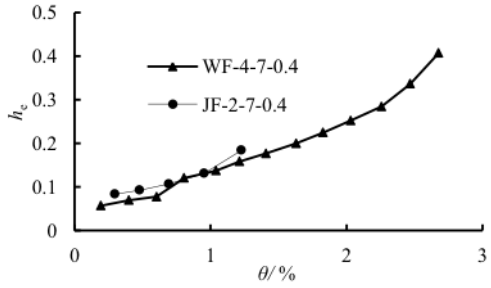

Fig. 7. Equivalent viscous damping coefficient

4. Conclusions

Specimen WF-4-7-0.4 occurs bending failure, and the hysteresis curve is full, the specimen has stronger energy dissipation ability and displacement ability, and the displacement ductility coefficient is greater than 3. The displacement of WF-4-7-0.4 is mainly composed of bending deformation, shear deformation and sliding deformation of plastic hinge region, which is about 90% of the total deformation. The bending deformation is about 70%∼80% of the total deformation. The specimens JF-2-7-0.4 occur shear bond failure, Its failure characteristics are that there are some vertical bond cracks in the intermediate longitudinal steel bar position of specimen, and the diagonal cracks development faster with the increase of the horizontal load, the diagonal cracks and vertical cracks intersect, so that the concrete falls off rapidly and the bearing capacity decreases sharply, and the specimen JF-2-7-0.4 has lower energy dissipation ability and displacement ability

References

[1] Y.H.Zhang, C.K.Huang, G.F.Zhao: *Using X-shaped reinforcing to improve anti-seismic capability of short columns.* Journal of Dalian University of Technology. *38* (1998),No.3, 332–336.

[2] Giovanni Minafo, F. Di Trapant, Giuseppina Amato: *Strength and ductility*

of RC jacketed columns:a simplified analytical method. Engineering Structures.*122* (2016),184–195.

[3] Kyoung-K.C, Gia.T.T, Jong.C.K: *Seismic performance of lightly shear reinforced RC columns.* Engineering Structures. *126* (2016),490–504.

[4] Haber.Z.B, Saiidi.M.S,Sanders.D.H: *Seismic Performance of Precast Columns with Mechanically Spliced Column-Footing Connections.* ACI Structural Journal. *111*(2014),No.3, 339–650.

[5] S.Q. He, R.X.An, L.Z.Song: *Effects of clip steel bar on failure modes of reinforced concrete columns under low cycle reversed loading.* China Civil Engineering Journal. *42* (2009),No.2, 17–23.

[6] Yan X, Henry W.Y: *Experimental studies on full-scale high-strength concrete columns.* ACI Structural Journal. *99* (2002),No.2,199–207.

[7] X.L.Lv, G.J.Zhang, S.L.Chen: *Research on seismic behavior of full-scale high-strength concrete frame columns with high axial compression ratios.* Journal of Building Structures. *30* (2009), No.3, 20–26.

[8] Z.B.Li, J.Song, X.L.Du, X.G.Yang: *Size effect of confined concrete subjected to axial compression.* Journal of Central South University. *21* (2014), 1217–1226.

[9] Jae-ii Sim, K.H.Yang, Kim H.Y, Choi B.J: *Size and shape effects on compressive strength of lightweight concrete.* Construction and Building Materials. *38* (2013), 854–864.

[10] S.T.Yi, E.K.Yang, J.C.Choi: *Effect of specimen sizes, specimen shapes, and placement directions on compressive strength of concrete.* Nuclear Engineering and Design. *236* (2006), No.2,115–127.

[11] J.R.Del Viso, J.R. Carmona, G. Ruiz: *Shape and size effects on the compressive strength of high-strength concrete.* Cement and Concrete Research. *38* (2008), No.3, 386–395.

[12] Kim J.E, Park W.S, Eom N.Y: *Size effect on compressive strength and modulus of elasticity in high performance concrete.* Advanced Materials Research. *634* (2013), No.1, 2742–2745.

[13] Y.F.Wang, H.L.Wu: *Size effect of concrete short columns confined with aramid FRP jackets.* Journal of Composites for Construction. *15* (2011), No.4, 535–544.

[14] Motaz M.E, Krauthammer.T: *Dynamic size effect in normal and high-strength concrete cylinders.* ACI Materials Journal. *102* (2005), No.2, 77–85.

[15] Sheikh S.A, Toklucu M.T: *Reinforced concrete columns confined by circular spiral and hoops.* ACI Structure Journal. *90* (1993), 542–553.

Received November 16, 2017